Talanta 115 (2013) 694–701

Contents lists available at SciVerse ScienceDirect

Talanta

journal homepage: www.elsevier.com/locate/talanta

Design and evaluation of an electrochemical immunosensor for measles serodiagnosis using measles-specific Immunoglobulin G antibodies

Philani Mashazi [a,b,*,1], Sibulelo Vilakazi [a,1], Tebello Nyokong [b,1]

[a] Nanotechnology Innovation Centre, Advanced Materials Division, Mintek, Private Bag X3015, Randburg 2125, South Africa
[b] Nanotechnology Innovation Centre, Sensors, Chemistry Department, Rhodes University, P.O. Box 94, Grahamstown 6140, South Africa

ARTICLE INFO

Article history:
Received 16 May 2013
Received in revised form
19 June 2013
Accepted 21 June 2013
Available online 28 June 2013

Keywords:
Measles-antigen
Measles-specific antibodies
Horse-radish peroxidase
Labeled-detection
Immunosensors

ABSTRACT

The design of electrochemical immunosensors for the detection of measles-specific antibodies is reported. The measles-antigen modified surface was used as an antibody capture surface. The detection of measles-specific IgG antibodies was accomplished using the voltammetric method and horse-radish peroxidase (HRP) labeled secondary antibody (anti-IgG) as a detecting antibody. The potential applications of the designed immunosensor were evaluated in buffer and serum solutions. The immunosensor exhibited good linearity at concentrations less than 100 ng mL^{-1} with R^2=0.997 and the limit of detection of 6.60 ng mL^{-1} at 3σ. The potential application of the immunosensor was evaluated in the deliberately infected human and newborn calf serum samples with measles-IgG antibody mimicking real-life samples. The designed electrochemical immunosensor could differentiate between infected and un-infected serum samples as higher catalytic currents were obtained for infected serum samples.

© 2013 Elsevier B.V. All rights reserved.

1. Introduction

Measles virus (MV) is a single-strand ribonucleic acid virus belonging to *Morbillivirus* genus in the family of Paramyxoviridae. MV is highly infectious and deadly to children with adult infection rate relatively small compared to children. MV can be transmitted through large droplets from coughing and sneezing or direct contact with the nasal or throat secretions from an infected person [1]. Secondary infections by MV do occur and this makes the detection and monitoring of this virus very important. Eastern and southern African countries have recently reported the resurgence of measles outbreaks with 200,000 confirmed cases and 1400 recorded deaths according UNICEF/WHO [2,3] and Centers for Disease Control and Prevention [4]. Confirmed measles cases have also been reported in various countries and regions worldwide making this a global problem [5–10]. South Africa has recently experienced various disease outbreaks, such as rift-valley fever (a zoonotic disease) with 13,902 confirmed animal cases (8581 deaths) [11] and measles with >17,000 confirmed human infected cases [11–13]. The complications of measles-HIV co-infections were reported during the outbreak [13]. The treatment of measles on HIV infected individuals is slower due to compromised immune response and hence slow production of measles-specific antibodies. The slow production of measles-antibodies results in slowing measles treatment and the recuperating process [14–16]. However there are no adverse effects to measles vaccination or treatment in HIV-infected individuals [17,18].

Serological testing methods for measles diagnosis monitor the production of Immunoglobulin M (IgM) [19–23], Immunoglobulin G (IgG) [19–21,24,25] and the presence of measles virus [23,26]. Commercially available systems widely used for measles serodiagnosis are based either on enzyme immunoassays (EIAs) or polymerase chain reactions (PCRs). Enzyme-linked immuno-sorbent assays (ELISAs) are the preferred system. IgM antibodies are the first antibodies produced in early stages of measles virus infection and disappear after almost 5 weeks. Therefore, they have been accepted as markers for recent or acute measles virus infections. On the other hand, IgG antibodies are the secondary produced antibodies and are known to persist long after the infection or immunization [21]. When IgG is used for serodiagnosis of measles, an increase in IgG antibody titer indicates an acute measles infection whilst stable levels of IgG antibody indicates convalescent stage of measles infection [27,28]. To evaluate whether the antibody titer are increasing, decreasing or remaining the same,

* Corresponding author at: Nanotechnology Innovation Centre, Advanced Materials Division, Mintek, Private Bag X3015, Randburg 2125, South Africa.
Tel.: +27 11 709 4497; fax: +27 11 709 4480.
E-mail addresses: philanim@mintek.co.za, philanimashazi@yahoo.com (P. Mashazi).
[1] ISE member.

0039-9140/$ - see front matter © 2013 Elsevier B.V. All rights reserved.
http://dx.doi.org/10.1016/j.talanta.2013.06.036

quantitative measurements are required. Electrochemical systems are useful in quantifying the level of analytes in the test samples. For serodiagnosis of measles using IgG antibodies, the differentiation can be obtained by measuring two samples obtained 2 weeks apart.

Several reports have demonstrated the efficiency of detecting measles-specific antibodies [19–25] using ELISA techniques. The limitations of ELISA methods are that they are laboratory centralized, time consuming, require bulk equipment for analysis and require skilled personnel for sample analysis and results interpretation. These ELISA requirements make the technique not applicable for remote applications at locations where outbreaks sometimes occur. There is therefore a need to investigate systems for serological diagnosis of measles on-site, i.e. outside the laboratory confinements with ease of results interpretation. Amongst the systems widely investigated are the dip-sticks or point-of-care (POC) assay test kits, such as the immunochromatographic or lateral flow test kits [29,30] which give qualitative results. Other systems that are of considerable interest are the electrochemical-based detection systems because they offer both qualitative and quantitative results. Glucose biosensor systems are the most widely used based on the electrochemical signal for detection and monitoring glucose in diabetic patients [31].

Electrochemical detection can also be incorporated into ELISA systems to make detection easier. The ease with which the electrochemical signal can be analyzed makes these the system of choice for serodiagnosis and monitoring of disease and virus outbreaks at remote locations. The electrochemical systems can be miniaturized for ease of portability which allows for their use at remote areas and for field-testing. The use of electrochemical detection of immuno reactions using HRP and its substrates has been widely studied and recently reviewed [32]. In this work, the horse-radish peroxidase (HRP) labeled anti-IgG was used to monitor (electrochemically) the specific interaction between measles-antigen (MAg) and measles-specific antibody (IgG isotype) mimicking the ELISA method. To increase the knowledge in this interesting field of scientific research, the design and application of electrochemical ELISA for measles serodiagnosis using measles-specific IgG antibodies will be reported. Serodiagnosis of measles using electrochemical ELISA is therefore reported here for the first time and the use of serum samples was included to mimic the real-life samples.

2. Experimental

2.1. Materials and supplies

Measles antigen (Rubeola Edmonston strain, R9750, MAg) and anti-Rubeola primary polyclonal antibody (R9750-10, IgG isotype, 1°PAb) were purchased from USBiologicals (USA) and required dilutions were performed before use. Peroxidase (HRP) conjugated anti-IgG secondary polyclonal antibody (611-703-127, 2°PAb) was purchased from Rockland (USA) and serial dilutions prepared as per experimental requirement. Acetonitrile (ACN), glutaraldehyde (GA), absolute ethanol, 3,3′,5,5′-tetramethylbenzidine (TMB, T0440) solution for ELISA experiments were purchased from Sigma-Aldrich (South Africa) and used as received. Bovine serum albumin (BSA) was purchased from Sigma-Aldrich and 2% BSA was prepared and used as the blocking buffer. Phosphate buffer saline (PBS) containing 8.0 g sodium chloride, 1.3 g dibasic sodium phosphate (Na_2HPO_4), 0.2 g monobasic sodium phosphate (NaH_2PO_4) in 1.0 L of distilled water (pH 7.4) was used. Solvents were distilled and dried before use. H_2O_2 (32%) was purchased from SAARChem (South Africa). Ultra-pure water was obtained from a Milli-Q water system (Millipore Corp. Bedford, MA, USA) and was used throughout the experiments.

2.2. Apparatus and methods

All electrochemical experiments were carried out using a computer-controlled Autolab Potentiostat/Galvanostat PGSTAT 302N (Eco Chemie, Utrecht, The Netherlands) driven by the General Purpose Electrochemical Systems (GPES) data processing software. The electrochemical data was collected using a gold electrodes (Au, $r=0.8$ mm) as working electrodes, platinum wire as counter electrode and silver|silver chloride (Ag|AgCl) 3 M NaCl solution as reference electrode. The 4-(2-aminoethyl) benzene diazonium (AEBD) salt used for electrochemical grafting was synthesized and purified as previously reported [33,34]. The covalent attachment of the MAg as a sensing element or capture protein was accomplished following a previously reported method [35]. Briefly, the gold electrode (Au) modification was achieved by first grafting the amine functionalized monolayer. Prior to modification, the electrode was cleaned thoroughly following the reported method [36,37]. The electrode modification was achieved by electrochemical grafting 1 mmol L^{-1} AEBD salt in acetonitrile solution containing 1 mmol L^{-1} $TBABF_4$ as an electrolyte to form phenylethylamino (PEA) monolayer. The PEA modified gold surface was then activated by immersing it in 5% GA in absolute ethanol solution for 1 h. The GA activated surface was represented as Au–PEA–GA. The immobilization of MAg was accomplished by immersing the GA activated electrode onto measles-antigen solution (20 μg mL^{-1}) and incubated at 4 °C overnight. The non-specific binding of amine reactive sites were blocked by incubating the measles-antigen modified electrode in 2% BSA solution at 37 °C for 1 h, the electrode was represented as Au–PEA–GA–MAg/BSA. After each incubation or immobilization step, washing with PBS-T was conducted three times to remove the physically adsorbed species. The modified surfaces were then stored in PBS-T containing 2% BSA at 4 °C before use.

3. Results and discussions

3.1. Enzymatic activity of HRP bound onto the 2°PAb, i.e. HRP-2°PAb

The activity of the HRP bound to the secondary antibody (HRP-2°PAb) was investigated for its activity to convert TMB to its oxidation products. The conversion of TMB to its oxidation products resulted in color changes from clear solution to blue and this was monitored by the UV–vis spectroscopy. Fig. 1 shows UV–vis spectral changes of HRP-2°PAb (0.10 μg mL^{-1}), (a) in the presence of H_2O_2 and (b) after introducing TMB.

The HRP preferably binds to the activated oligosaccharides on the Fc region of the antibody [38] leaving the Fab region for further reactions with antigen. This binding even is however uncontrollable but the studies have shown that the antibodies conjugated following this method are still applicable, i.e. they retain both the enzyme and the antibody activity [39–41]. During this binding the reactive HRP site remains unperturbed and this was observed by the unchanged spectrum of HRP (alone) when compared to antibody bound HRP. Both spectra showed an intense Soret B band (at 401 nm) and weak Q band around 630 nm typical of HRP enzyme consisting of the redox active iron(III)pophyrin-like molecule [42], Fig. 1(a)(i). After the addition of H_2O_2, the 11 nm bathochromic shift in the Soret B band absorption peak was observed from 401 nm (red spectrum) to 412 nm (blue spectrum) in Fig. 1(a). The shift in the B band absorption peak was attributed to the change in HRP oxidation states from +3 to +5, Fig. 1(a). The spectral changes confirm the oxidation of HRP by H_2O_2 and the reduction of H_2O_2. Fig. 1(b) shows the spectral changes before (i, blue), during (dotted-dash) and (ii) after (ii, red) the introduction of TMB into an activated HRP (+5) solution. The spectral

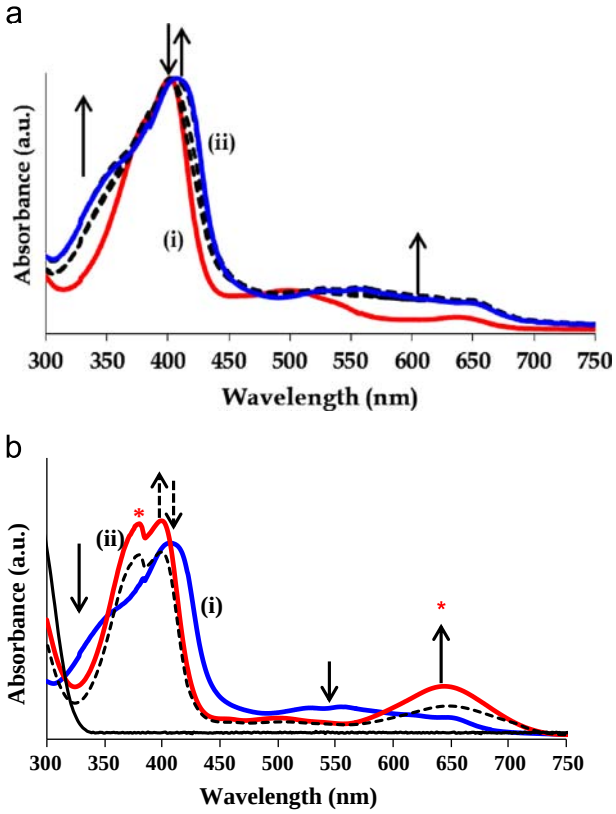

Fig. 1. UV–vis spectral changes of (a) 0.1 mg mL^{-1} (HRP)-2°Ab (i) before and (ii) after 10 min in the presence of 20 μmol L^{-1} H_2O_2 and (b) (i) before and (ii) after addition of 20 μg mL^{-1} TMB. The spectrum (i) is the same as (ii) in (a).

changes in Fig. 1(b) shows the shift of the Soret band absorption band for the HRP (+5) from 412 nm (i) back to its original position 401 nm (ii) for HRP (+3) oxidation state. The hypsochromic shift of the Soret absorption band to 401 nm was an indication of the reduction of HRP (+5) back to its native oxidation state of +3. The TMB was consequently oxidized and the absorption peaks at 389 nm and 650 nm (marked by asterisks) were an indication of TMB oxidation products. The solution turned blue in color indicating the oxidation of TMB to TMB oxidation products.

When the TMB was introduced to the HRP enzyme solution in the absence of H_2O_2, the spectrum observed was similar to that in Fig. 1(a)(i) showing only the HRP absorption peak. TMB alone does not show any absorption peak when in solution [43] and within the studied UV–vis window, i.e. 300–900 nm as shown in Fig. 2(b, solid black spectrum). Clearly this experimental investigation confirms the activity of the HRP on the HRP-2°PAb and also the oxidation of TMB. It also further confirms that the oxidation of TMB only occurs in the presence of H_2O_2 which initializes the enzymatic activity towards TMB. The monitoring of the presence of measles-specific 1°PAb has been accomplished using reported spectrophotometric detection via indirect immunoassays protocols [19,20,44]. Spectrophotometric detection systems are laboratory confined and therefore research is ongoing into electrochemical detection systems which offer onsite monitoring. A few studies have already shown that electrochemical methods can be employed in the monitoring blue TMB oxidation products generated by HRP enzymatic catalysis [45–47].

In the recently published work, we have demonstrated that impedance spectroscopy can be used for the detection of measles-specific IgG antibodies using measles-antigen as capture protein [35]. The challenge faced in that work was that the measles antigen modified surface could not differentiate between the IgG

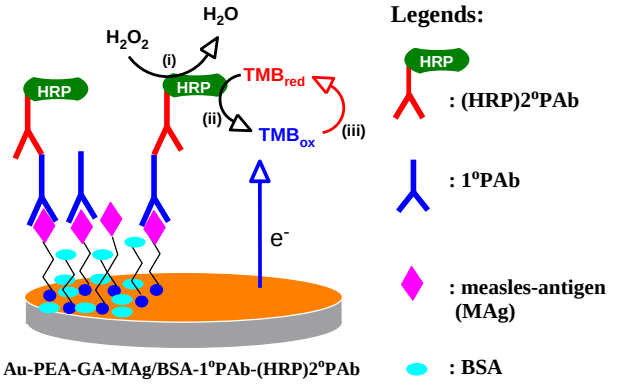

Fig. 2. Electrochemical immunoassay detection of measles-specific antibodies using HRP-labeled secondary antibodies (HRP-2°PAb).

and IgM antibodies. Both antibodies are produced during the acute measles infection and IgG sometimes signify long immunity to measles. Both these antibodies will be present in samples to be analyzed. This work then was set-out to address this drawback of the impedance study. The use of labeled secondary antibody specific to either IgM or IgG antibodies addresses this drawback. After the primary measles-specific IgG binds specifically to measles antigen, the enzyme (HRP) labeled anti-IgG secondary antibody (HRP-2°PAb) is introduced and the detection then take place. This might compromise on the sensitivity of the designed electrochemical immunosensor. The amount of IgG antibodies in bodily fluids is higher (80%) than other antibodies with IgM (6%) as third highest produced antibody.

The measles-specific 1°PAb (IgG) antibody detection was accomplished by first immersing the MAg modified sensor electrodes in the antibody infected solution or measles infected/suspected sample followed by thorough rinsing with PBS-T. After that the measles-specific IgG captured electrode was immersed in the HRP-2°PAb solution for detection and rinsed further. The detection was conducted in H_2O_2+TMB solution. Fig. 2 shows the detection principle for the designed electrochemical immunoassay with step labeled (iii) showing the electrochemical detection.

3.2. *Electrochemical detection of measles-specific IgG antibodies using HRP-2°PAb*

The electrochemical detection on an electrode bearing HRP-2°PAb was performed in solution containing 20 μmol L^{-1} H_2O_2 and 20 μg mL^{-1} TMB as a substrate as illustrated in Fig. 2(iii). Electrochemically, the presence of the enhanced signal due to TMB electrocatalysis indicates an infected or measles seropositive sample. This means that the binding between MAg-1°PAb–(HRP) 2°PAb has occurred and the electrode is represented as Au–PEA–GA–MAg/BSA-1°PAb–(HRP)2°PAb. The lack of detectable signal signifies the negative sample; the electrode stays the same and represented as Au–PEA–GA–MAg/BSA. Electrochemical analysis using cyclic voltammetry was used in this study to monitor and detect the amount of enzymatic products thus substituting the spectrophotometric analysis. Different modified electrodes were investigated for their electrochemical response toward H_2O_2 and TMB solutions. Since the enzymatic oxidation of TMB requires the presence of H_2O_2, the detection solution contained H_2O_2 and TMB. Fig. 3 shows the (a) cyclic voltammograms and corresponding (b) bar chart (showing current responses) of 20 μmol L^{-1} H_2O_2+ 20 μg mL^{-1} TMB solution at various electrode surfaces, (i) bare Au, (ii) Au–PEA, (iii) Au–PEA–GA–MAg/BSA, (iv) Au–PEA–GA–MAg-1°PAb and (v) Au–PEA–GA–MAg/BSA-1°PAb–(HRP)2°PAb.

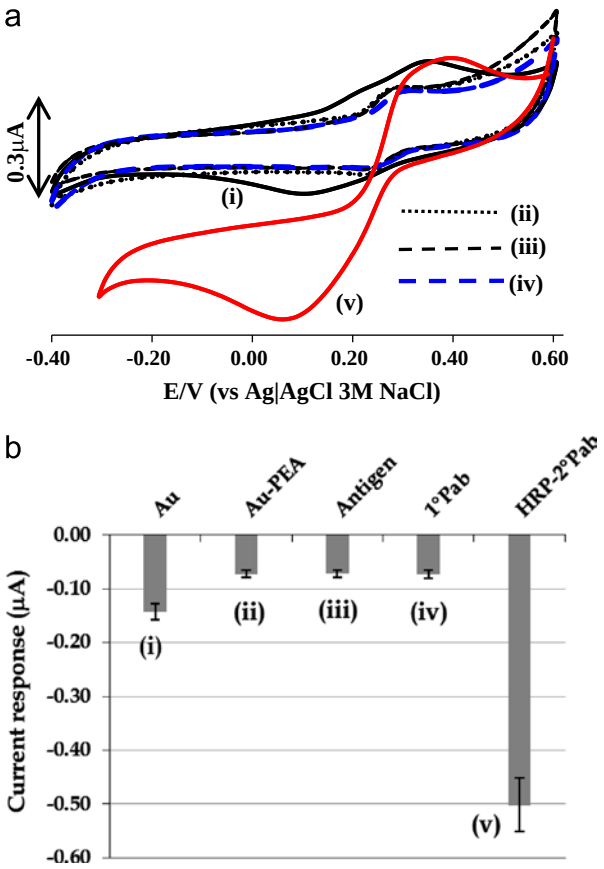

Fig. 3. (a) Cyclic voltammograms and (b) catalytic current (bar chart) of (i) Au, (ii) Au–PEA, (iii) Au–PEA–GA–MAg/BSA, (iv) Au–PEA–GA–MAg/BSA-1°PAb and (v) Au–PEA–GA–MAg/BSA-1°PAb–(HRP)2°PAb. All the electrodes were measured in PBS (pH 7.4) containing 20 μg mL^{-1} TMB+20 μmol L^{-1} H_2O_2. The number of experiments (n)=3, %RSD≤6.0% for all the electrodes studied.

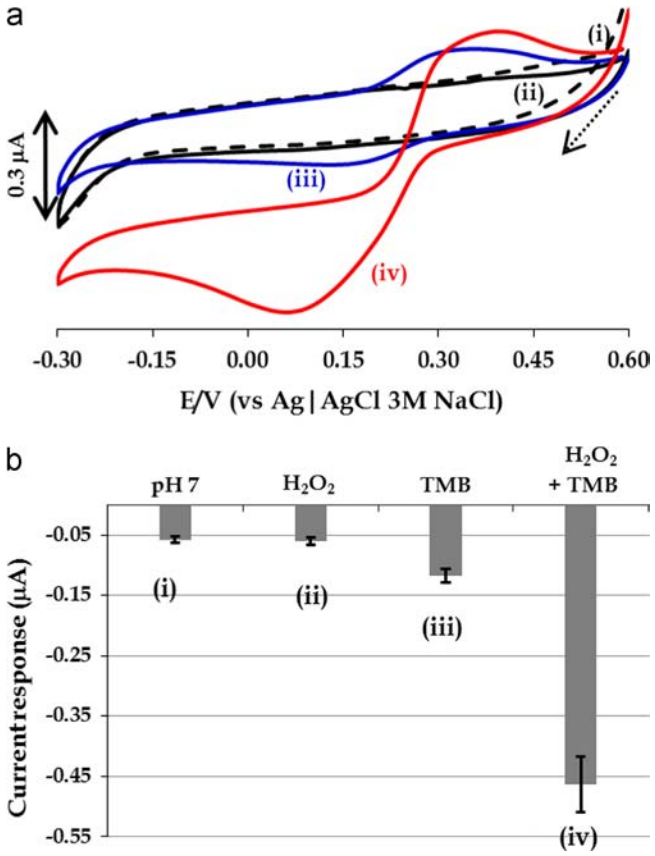

Fig. 4. Cyclic voltammograms of (a) Au–PEA–GA–MAg/BSA-1°PAb–(HRP)2°PAb in (i) pH 7.4 (black dotted), (ii) 20 μmol L^{-1} H_2O_2 (black solid), (iii) 20 μg mL^{-1} TMB (blue) and (iv) 20 μg mL^{-1} TMB+20 μmol L^{-1} H_2O_2 (red) and (b) bar chart showing the comparative current response at various detecting solutions. The number of experiments (n)=3, %RSD≤5.0% for all the electrodes studied. (For interpretation of the references to color in this figure legend, the reader is referred to the web version of this article.)

A higher increase in catalytic current response was observed on the electrode modified with (HRP)2°PAb, in Fig. 3(v). The bare gold electrode showed a broad split redox peaks due to TMB at the investigated concentrations. The observed redox peaks due to TMB was suppressed at (ii) Au–PEA, (iii) Au–PEA–GA–MAg/BSA and (iv) Au–PEA–GA–MAg/BSA–1°PAb electrodes. This suppression of the TMB peak was a confirmation of electrode modification and the immobilization of various layers onto an electrode surface. It was interesting to note that the TMB redox couple did not disappear completely and this signifies the permeability of the immobilized layers to TMB. The cyclic voltammograms due to Au–PEA–GA–MAg/BSA-1°PAb–(HRP)2°PAb modified electrode gave enhanced TMB reduction catalytic currents. The enhanced electro-reductive currents have also been reported in literature [48]. This increase in catalytic reductive currents confirms HRP electrocatalysis towards TMB in the presence of H_2O_2 which initializes the enzymatic process as shown in Fig. 2. The TMB electro-reductive currents due to TMB were much higher and this was attributed to higher molar concentrations of oxidized TMB products from the enzymatic reactions. The results were studied in triplicate for each modified surface. The percentage relative standard deviation (%RSD) was ≤6.0% for all the electrodes signifying good variation of each surface modification.

The effect of the detection solution on an Au–PEA–GA–MAg/BSA-1°PAb–(HRP) 2°PAb electrode was investigated. Higher reductive catalytic currents in Fig. 3(v) were observed. Therefore, at this electrode we studied the contribution from each component of the detection solution. Fig. 4 shows (a) cyclic voltammograms and (b) their corresponding bar chart showing the comparative current response during the electrochemical measurement of Au–PEA–GA–MAg/BSA-1°PAb–(HRP)2°PAb in different solutions (i) PBS (pH 7.4), (ii) PBS (20 μmol L^{-1} H_2O_2), (iii) PBS (20 μg mL^{-1} TMB) and (iv) PBS (20 μmol L^{-1} H_2O_2+20 μg mL^{-1} TMB).

Fig. 4(a)(i) in buffer alone and (ii) in 20 μmol L^{-1} H_2O_2, showed just background currents with no electroactive redox peak observed within the studied potential window. We only observed an increase in currents at −0.2 V and above. When the electrode was introduced to PBS containing 20 μg mL^{-1} TMB in Fig. 4(a)(iii), a broad redox peak was observed at $E_{1/2}$=+0.20 V. The use of PBS solution containing 20 μg mL^{-1} TMB and 20 μmol L^{-1} H_2O_2 in Fig. 4 (a)(iv) resulted in enhanced catalytic reduction currents. The enhancement in the catalytic reduction peak currents has been shown before when HRP-labeled detection was utilized [46]. The respective catalytic current responses are shown in Fig. 4(b) in a bar chart. Clearly from the bar chart, enhanced catalytic reduction currents were observed for the mixed H_2O_2 and TMB detecting solution. The importance of H_2O_2 for the initial enzymatic step is clearly demonstrated, as the catalytic current in the presence of TMB alone was very small when compared to when both H_2O_2 and TMB were used. For real sample analysis, the enhancement in catalytic reductive current will only be observed if the sample has measles-specific IgG antibodies and hence the binding of the HRP-2°PAb. When the measles-specific IgG antibodies are not present, the electrode cyclic voltammograms remain the same as those in Fig. 3(iii). The effect of the detection solution on the analytical signal showed that the presence of both H_2O_2 and TMB results in an enhancement of the catalytic reduction peak at HRP(2°PAb) surfaces. The solution study results were conducted in triplicate

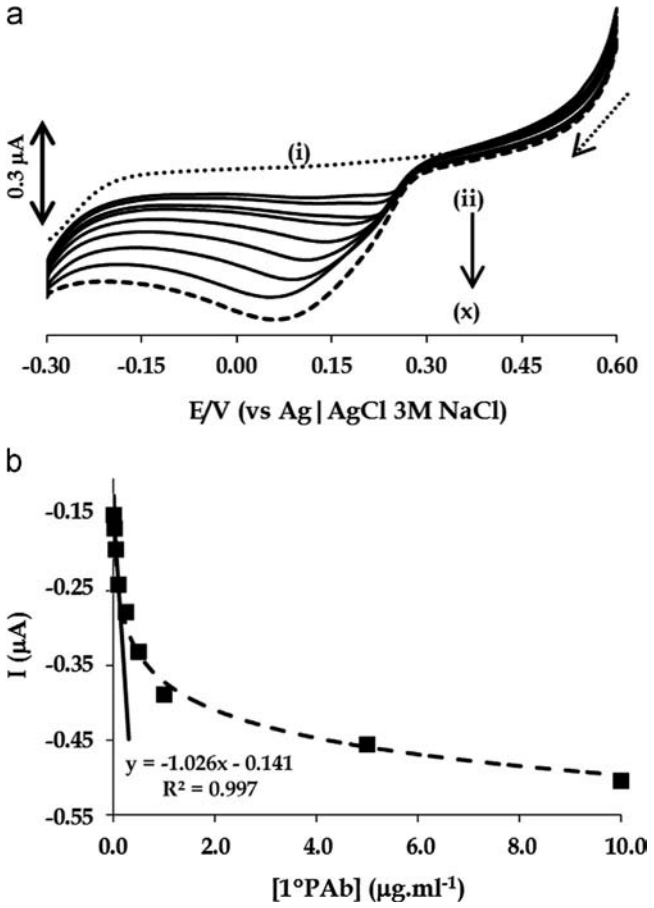

Fig. 5. (a) Cyclic voltammograms (forward scan only for clarity) showing the variation of antibody (1°PAb) concentrations ranging from (i) 10 ng mL^{-1} to (x) 10 μg mL^{-1} and (b) plot of currents I (nA) vs. [1°PAb] (μg mL^{-1}) from the data obtained in (a). The electrode used is Au–PEA–GA–MAg/BSA. The detecting antibody [HRP-2°PAb] = 50 μg mL^{-1} and the detecting solution was pH 7.4+20 μg mL^{-1} TMB+20 μmol L^{-1} H_2O_2.

for each solution at Au–PEA–GA–MAg/BSA-1°PAb–(HRP) 2°PAb. The percentage relative standard deviation (%RSD) for all the solutions was ≤5.0% signifying very good variation of each surface modification and solution. The performance of the electrochemical immunosensor at varied measles-specific IgG (1°PAb) concentrations was evaluated.

3.3. Performance of the immunosensor at varied antibody (1°PAb) concentrations

The performance of the immunosensor at varied antibody (1°PAb) concentrations ranging from 10 ng mL^{-1} to 10 μg mL^{-1} was studied. The MAg/BSA modified electrode surface was incubated in different concentrations of 1°PAb. The electrodes were then washed with PBS-T and then incubated in the solution containing HRP-2°PAb (50 μg mL^{-1}). The cyclic voltammograms were then recorded in PBS solution containing H_2O_2 and TMB. Fig. 5 shows (a) the cyclic voltammograms (forward scan only for clarity) recorded during the variation of antibody (1°PAb) concentrations ranging from (i) 10 ng mL^{-1} to (x) 10 μg mL^{-1}; (b) shows the plot of catalytic current (I/nA) vs. [1°PAb] μg mL^{-1}.

The increase in catalytic reduction peak currents occurred at increasing antibody concentrations as shown in Fig. 5(a). The dependence of the catalytic peak currents on antibody concentrations gave a dose response curve shown in Fig. 5(b). The linear dynamic concentration range was observed between 10 and 100 ng mL^{-1}, the linear regression equation was i_p (μA) = −0.141 to 1.026 [1°PAb]. The correlation coefficient (R^2) of 0.997 was obtained. The catalytic peak currents dependence showed a dose response curve with a plateau at concentrations higher than 100 ng mL^{-1}. The plateau of the dose response curve indicates saturation of an antigen (MAg) modified surfaces as the concentrations for 1°PAb increased above 100 ng mL^{-1}. The dose response curve was similar to that obtained for the ELISA experiments [35]. In that study, an increase in optical density (OD) due to the increasing 1°PAb concentrations was observed and formed a plateau at much higher 1°PAb concentrations. The limit of detection (LoD) for the electrochemical measles immunosensor was found to be 6.60 ng mL^{-1} calculated using the 3σ method. The obtained LoD was comparable to the reported values for other human IgG detection [48]. Electrochemical detection gives both qualitative and quantitative results. Both results are useful in the measles serodiagnosis, especially when using measles-IgG antibodies. Fig. 5 shows, without a doubt, the linear dependence of catalytic reduction peak currents on the antibody (1°PAb) concentrations at concentrations ranging from 10 to 100 ng mL^{-1}. Serodiagnosis of acute and convalescent measles infections require monitoring the increase in IgG antibody concentrations and that the samples must be obtained 2 weeks apart [27,28]. The increase in measles-specific IgG (1°PAb) antibody titers indicates the acute or recent measles infections. The decrease or stable measles-specific IgG antibody titers therefore indicates convalescent stages of the measles infections.

3.4. Human and newborn calf sera studies

The newborn calf serum (NCS) and human serum (HS) were used to investigate the applicability of the designed measles electrochemical immunosensor towards detecting measles-specific IgG antibodies. The measles-antigen modified gold electrodes were incubated into either 0.1% HS or 0.1% NCS solutions followed by thorough rinsing with PBS-T (pH 7.4). The electrodes were further incubated into the HRP-2°PAb solution followed by thorough rinsing again. Scheme 1 shows the detection of antibodies (1°PAb) in seropositive or negative 0.1% HS and 0.1% NCS solution. After the incubation steps, the electrochemical measurements (cyclic voltammograms) were carried out in PBS (pH 7.4) solution containing 20 μmol L^{-1} H_2O_2 and 20 μg mL^{-1} TMB.

After the immunoassay steps in Scheme 1, the electrochemical measurement was carried out. Fig. 6 shows the (a) cyclic voltammograms and (b) bar chart (catalytic peak currents) of Au–PEA–GA–MAg/BSA electrodes (i) before and after (ii) incubating in the 0.1% HS pH 7.4 buffer solution, (iii) 0.1% HS infected with 1°PAb (5.0 μg mL^{-1}) and (iv) blocked/inhibited 0.1% HS with 5.0 μg mL^{-1} MAg. All the electrodes were incubated in the (HRP)2°PAb solution before electrochemical measurements.

The electrode (Au–PEA–GA–MAg/BSA) in Fig. 6(a)(i) showed very small redox couple with small currents due to TMB. After the electrode was introduced into 0.1% HS, in Fig. 6(a)(ii) an increase in the reduction currents was observed. This increase in reduction currents was attributed to the binding of antibodies available in HS solution onto the MAg/BSA on the electrode. The control study with only BSA immobilized onto the electrode surface exhibited current response similar to those of the MAg/BSA electrodes, in Fig. 6(i), clearly indicating that the binding was on the MAg. Furthermore, the presence of the electrochemical signal at MAg/BSA modified electrode surfaces confirmed that the binding occurred with anti-IgG HRP secondary antibodies, i.e. (HRP) 2°PAb. Therefore the binding molecule to the antigen (MAg) could possibly be an IgG type biomolecule and it further binds anti-IgG HRP, selectively. Additional experiments where 0.1% HS was deliberately infected with 1°PAb (5.0 μg mL^{-1}), in Fig. 6(a)(iii) resulted in even higher reduction currents. This was attributed

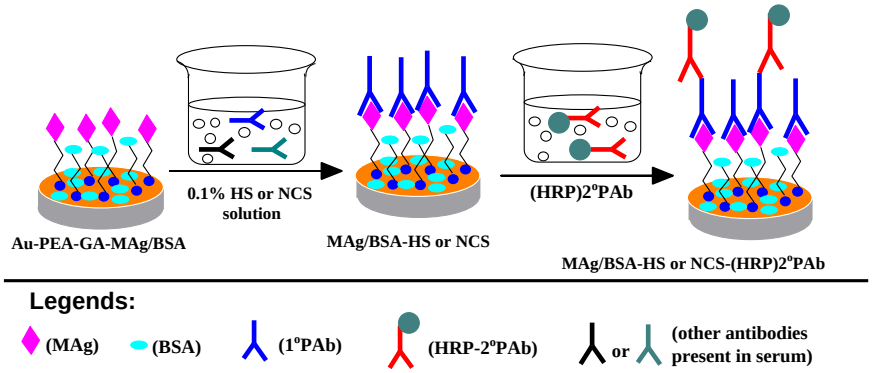

Scheme 1. Schematic representation of the detection principle for 1°PAb in 0.1% HS and 0.1% NCS sample matrix.

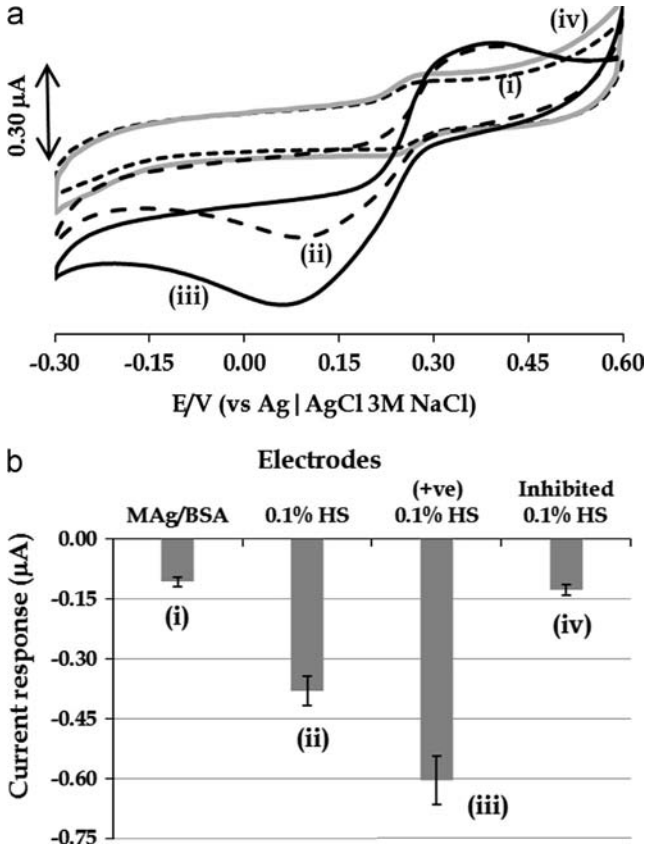

Fig. 6. (a) Cyclic voltammograms and (b) bar chart (current response) of Au–PEA–GA–MAg/BSA electrode (i) as prepared and after immersing in (ii) 0.1% HS pH 7.4 buffer, (iii) 0.1% HS deliberately infected with 1°PAb (5 µg mL^{-1}) and (iv) inhibited 0.1% HS with 5 µg mL^{-1} antigen. All in the presence of [HRP-2°PAb] (50 µg mL^{-1}) and measured in pH 7.4 solution containing 20 µg mL^{-1} TMB +20 µmol L^{-1} H_2O_2. +ve 0.1% HS=0.1% HS+5 µg mL^{-1} 1°PAb. The number of experiments (n)=3, %RSD≤5.7% for all the HS serum samples.

to the presence of 1°PAb in addition to the already present species (possibly IgG) that bind to MAg and (HRP)2°PAb.

To confirm that the observed increase in current at 0.1% HS was due to species in HS binding onto the MAg, the blocking or inhibition was conducted. The MAg (5.0 µg mL^{-1}) was injected into 0.1% HS solution and the reaction was allowed to stand for 20 min at room temperature. Afterwards the electrode (Au–PEA–GA–MAg/BSA) was incubated in the inhibited solution for an hour, transferred into HRP-2°PAb and transferred to detection solution. The recorded cyclic voltammogram, Fig. 6(a)(iv), shows the drastic decrease in catalytic currents (almost similar to the electrode with the MAg/BSA, i.e. Au–PEA–GA–MAg/BSA) for the inhibited solution. This clearly indicates that in HS solution there are IgG proteins capable of binding both antigen (MAg) and anti-IgG HRP (2°PAb-HRP). The presence of IgG antibody in HS solution is attributed to long lasting humoral immunity to measles. This was not surprising as measles infections are targeted for global eradication by World Health Organization (WHO) through Expanded Program on Immunization (EPI). Such initiatives by WHO makes the presence of vaccines to measles widely available. A study conducted in 2001 confirmed that IgG antibodies specific to measles persists long after the infection or immunization [21]. Therefore, this explains the presence of measles-specific IgG antibodies and anti-IgG secondary antibodies in human serum. Even after such extensive WHO-EPI program for measles eradication, these programs never reach 100% of the population and this leads to the disease resurgence. In the recent past, there was a resurgence of measles with confirmed cases reported in various countries and regions worldwide making this a global problem [5–10]. In the southern Africa, the resurgence of measles virus infection accompanied with high HIV prevalence makes measles diagnosis and treatment of high importance [4,13,49,50]. This investigation further highlighted the importance of patient information prior to sample diagnosis so as to avoid misdiagnosis. Fig. 6(b) shows the relative catalytic peak currents obtained from the cyclic voltammograms in Fig. 6(a) for various electrodes after detection. The samples were measured in triplicate and %RSD for all the samples was ≤5.8% and showing good reproducibility and less variation from sample-to-sample.

The newborn calf serum (NCS) was also investigated for comparison with the human serum studies. Fig. 7 shows the (a) cyclic voltammograms and (b) bar chart (comparative catalytic peak currents) of Au–PEA–GA–MAg/BSA electrode (i) before and after incubation in (ii) 0.1% NCS and (iii) 0.1% NCS deliberately infected with 1°PAb (5.0 µg mL^{-1}). All the electrodes were incubated in HRP-2°PAb (50 µg mL^{-1}) prior to being transported into the detection solution. The negative serum (−ve NCS) refers to 0.1% NCS solution alone and positive serum (+ve NCS) refers to 0.1% NCS infected deliberately with 5.0 µg mL^{-1} antibody (1°PAb) solution to mimic an infected sample.

The electrodes with the MAg/BSA and 0.1% NCS alone, in Fig. 7 (a)(i and ii) gave almost similar cyclic voltammograms with no noticeable catalytic peak currents. The lack of observable increase reduction currents clearly shows that there is no interfering species with the measles-antigen in the negative serum (−ve NCS). However, when the serum 0.1% NCS was deliberately infected with the 5.0 µg mL^{-1} 1°PAb (+ve NCS), the increase in current was observed as shown in Fig. 7(a)(iii). The increase in catalytic currents is a confirmation that the electrodes can selectively detect the antibodies in the complex NCS sample matrix. The studies were conducted in triplicate and the %RSD for all the NCS samples was ≤8.5% showing good reproducibility and less

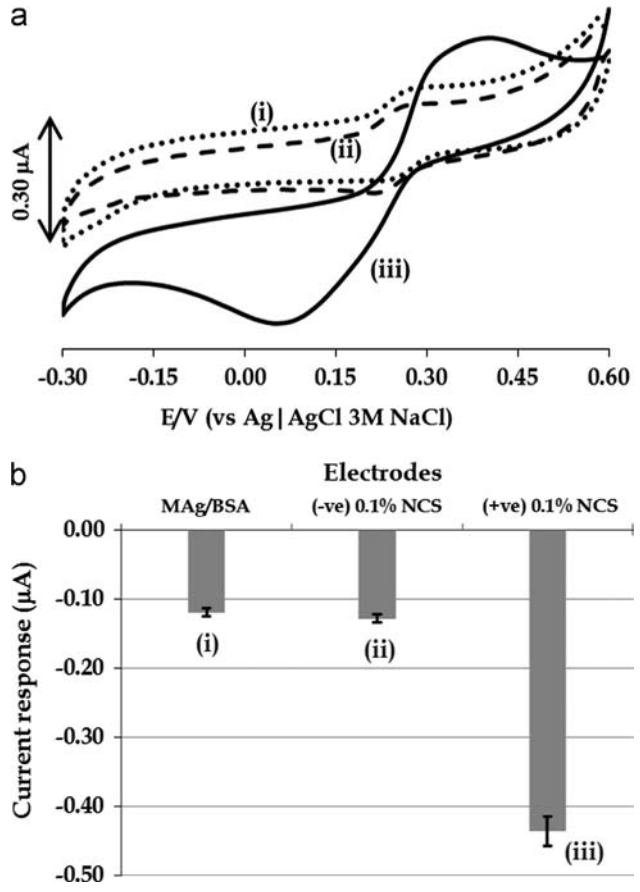

Fig. 7. (a) Cyclic voltammograms and (b) bar chart (comparative current response) of Au–PEA–GA–MAg/BSA electrode (i) before and after immersing in (ii) 0.1% NCS pH 7.4 buffer (−ve 0.1% NCS) and (iii) 0.1% NCS deliberately infected with 1°PAb 5.0 μg mL^{-1} (+ve 0.1% NCS). Analysis was conducted after binding of [HRP-2°PAb] (50 μg mL^{-1}) and measurement in pH 7.4 solution containing 20 μg mL^{-1} TMB +20 μmol L^{-1} H_2O_2. The number of experiments (n)=3, %RSD≤8.5% for all the NCS samples studied.

variation. The studies conducted in this present work clearly show the potential use of these electrochemical immunosensor systems for the detection of measles-specific IgG antibodies. Furthermore, these immunosensor systems can also be used for surveillance of disease and virus outbreaks at remote locations due to the fact that electrochemical systems can be miniaturized for ease of portability. It would have been interesting to study the infected blood samples but these are not readily availability. Furthermore, there are strict regulatory protocols for obtaining the blood infected samples. However, we had used human serum and new born-calf serum to demonstrate the applicability of the electrochemical immunosensor. The results were convincing in that we managed to detect measles-specific IgG antibodies in very complex serum samples.

4. Conclusions

In conclusion, this work demonstrated the design of an electrochemical ELISA immunosensor using the intimate and covalent immobilization of measles-virus antigen (MAg) onto gold electrode surface. The detection of measles-specific IgG antibodies (1°PAb) was shown to be possible using HRP labeled anti-IgG (2°PAb) following an indirect electrochemical immunoassay. The designed immunosensor for measles diagnosis was applicable in human and newborn calf sera. The detection in human serum showed the need for the knowledge or history of the patient so as to avoid misdiagnosis. Good limit of detection (6.60 ng mL^{-1}) was obtained and this was equivalent to electrochemical immunoassays for the detection of human-IgG antibodies. Monitoring both qualitative and quantitative antibody concentration was possible and the use of enzyme labeled secondary antibodies may assist in cases of discriminating which antibody isotype is detected, i.e. IgG (using anti-IgG-HRP) or IgM (using anti-IgM-HRP). This study will constitute the main thrust of our future investigation.

Acknowledgments

This work was supported by Mintek through Department of Science and Technology (DST)/Mintek Nanotechnology Innovation Centre (NIC) and by National Research Foundation (NRF) through DST/NRF South Africa Research Chairs Initiative for Professor of Medicinal Chemistry and Nanotechnology as well as Rhodes University. PM would also like to thank NRF South Africa for financial support through Thuthuka Post-PhD Track Programme (TTK1207183385).

References

[1] WHO (World Health Organization), Department of Immunization, Vaccines and Biologicals, Switzerland, 2007.
[2] WHO (World Health Organization),UNICEF Joint Annual Measles Report, 2010.
[3] WHO (World Health Organization), WER 86, 2011, pp. 1–16.
[4] CDC (Center for Disease Control and Prevention), MMWR 60, 2011, pp. 374–378.
[5] K.E. Brown, M.N. Mulders, F. Freymuth, S. Santibanez, M.M. Mosquera, S. Cordey, J. Beirnes, S. Shulga, R. Myers, D. Featherstone, Euro Surveill., 16, 2011, 1–5, pii=19852. Available online: ⟨http://www.eurosurveillance.org/ViewArticle.aspx?ArticleId=19852⟩.
[6] N. Ramamurty, D. Raja, P. Gunasekaran, E. Varalakshmi, S. Mohana, L. Jin, J. Med. Virol. 78 (2006) 508–513.
[7] C. Kuroiwa, P. Vongphrachanh, P. Xayyavong, K. Southalack, M. Hashizume, S. Nakamura, J. Epidemiol. 11 (2000) 255–262.
[8] K. Vainio, K. Rønning, T.W. Steen, T.M. Arnesen, G. Ånestad, S. Dudman, Euro Surveill. 16, 2011, 1–3, pii=19804. Available online: ⟨http://www.eurosurveillance.org/ViewArticle.aspx?ArticleId=19804⟩.
[9] A.J. Vyse, N.J. Gay, J.M. White, M.E. Ramsay, R.W.G. Brown, B.J. Cohen, L.M. Hesketh, P. Morgan-Capner, E. Miller, Epidemiol. Rev. 24 (2002) 125–136.
[10] K.R. Ehresmann, N. Crouch, P.M. Henry, J.M. Hunt, T.L. Habedank, R. Bowman, K.A. Moore, J. Infect. Dis. 189 (Suppl. 1) (2004) S104–S107.
[11] NICD (National Institute of Communicable Diseases), Communicable Diseases Outbreaks, vol. 9, 2011, Available from: ⟨http://www.nicd.ac.za/⟩, 2011 (accessed November 2011).
[12] C. Albertyn, H. van der Plas, D. Hardie, S. Candy, T. Tomoka, E.B. LeePan, J.M. Heckermann, S. Afr. Med. J. 101 (2011) 313–317.
[13] D.M. le Roux, S.M. le Roux, J.J. Nuttall, B.S. Eley, S. Afr. Med. J. 102 (2012) 760–764.
[14] P. Waibale, S.J. Bowlin, E.A. Mortimer Jr., C. Whalen, Int. J. Epidemiol. 28 (1999) 341–346.
[15] V. de Carvalho, L.P. Marinoni, L.F. Martins, K. Taniguchi, C.R. da Cruz, J. Bertogna, J.F. Neto, Braz. J. Infect. Dis. 7 (2003) 346–352.
[16] P.F. Belaunzaran-Zamudio, M.L. Garcia-Leon, R.M. Wong-Chew, A. Villasis-Keever, J. Cuellar-Rodriguez, J.L. Mosqueda-Gomez, T. Munoz-Trejo, K. Escobedo, J.I. Santos, G.M. Ruiz-Palacios, J.G. Sierra-Madero, Vaccine 27 (2009) 7059–7064.
[17] L. Aurpibul, T. Puthanakit, T. Sirisanthana, V. Sirisanthana, Clin. Infect. Dis. 45 (2007) 637–642.
[18] R.F. Helfand, W.J. Moss, R. Harpaz, S. Scott, F. Cutts, Bull. World Health Organ. 83 (2005) 329–337.
[19] D.D. Erdman, L.J. Anderson, D.R. Adams, J.A. Stewart, L.E. Markowitz, W.J. Bellini, J. Clin. Microbiol. 29 (1991) 1466–1471.
[20] K.B. Hummel, D.D. Erdman, J. Heath, W.J. Bellini, J. Clin. Microbiol. 30 (1992) 2874–2880.
[21] M.B. Isa, L. Martinez, M. Giordano, M. Zapata, C. Passeggi, M.C. de Wolff, S. Nates, J. Clin. Microbiol. 39 (2001) 170–174.
[22] A. Uzicanin, I. Lebega, M. Nanuyja, S. Mercader, P. Rota, W. Bellini, R. Helfand, J. Infect. Dis. 204 (2011) S564–S569.
[23] V. Hutse, K. Van Hecke, R. De Bruyn, O. Samu, T. Lernout, T. Muyembe, B. Brochier, Int. J. Infect. Dis. 14 (2010) e991–e997.
[24] A. Chakravarti, D. Rawat, S. Yadav, Diag. Microbiol. Infect. Dis. 47 (2003) 563–567.
[25] M.A. Riddell, G.B. Byrnes, J.A. Leydon, H.A. Kelly, Bull. World Health Organ. 81 (2003) 701–707.
[26] B. Thomas, S. Beard, L. Jin, K.E. Brown, D.W.G. Brown, J. Med. Virol. 79 (2007) 1587–1592.

[27] P. Kutty, J. Rota, W. Bellini, S.B. Redd, Manual for the Surveillance of Vaccine-Preventable Diseases, in: S.W. Roush, L. McIntyre, L.M. Baldy (Eds.), Centers for Disease Control and Prevention, Atlanta, GA, 2011, pp. 7.1–7.16. (Chapter 7).
[28] C.-H. Pan, G.S. Jimenez, N. Nair, Q. Wei, R.J. Adams, F.P. Polack, A. Rolland, A. Vilalta, D.E. Griffin, Clin. Vacc. Immunol. 15 (2008) 1214–1221.
[29] T. Hosegawa, A. Asaeda, Y. Hamaguchi, K. Numazaki, Hybridoma 28 (2009) 241–249.
[30] L. Warrener, R. Slibinskas, K.B. Chua, W. Nigatu, K.E. Brown, K. Sasnauskas, D. Samuel, D. Brown, Bull. World Health Organ. 89 (2011) 675–682.
[31] A. Heller, B. Feldman, Acc. Chem. Res. 43 (2010) 963–973.
[32] F. Ricci, G. Adornetto, G. Palleschi, Elechim. Acta 84 (2012) 74–83.
[33] N. Kornblum, D.C. Ifflan, J. Am. Chem. Soc. 71 (1949) 2137–2143.
[34] S. Griveau, D. Mercier, C. Vautrin-Ul, A. Chausse, Electrochem. Commun. 9 (2007) 2768–2773.
[35] P.N. Mashazi, P. Tetyana, S. Vilakazi, T. Nyokong, Biosens. Bioelectron. 49 (2013) 32–38.
[36] D.L. Pilloid, X. Chen, P.L. Dutton, C.C. Mosser, J. Phys. Chem. B 104 (2000) 2868–2876.
[37] D. Losic, J.J. Gooding, J.G. Shapter, Langmuir 17 (2001) 3307–3316.
[38] T. Mizuochi, T. Taniguchi, A. Shimizu, A. Kobata, J. Immunol. 129 (1982) 2016–2020.
[39] G.B. Wisdom, Clin. Chem. 22 (1976) 1243–1255.
[40] P.K. Nakane, A. Kawaoi, J. Histochem. Cytochem. 22 (1974) 1084–1091.
[41] S.E. Winston, S.A. Fuller, M.J. Evelegh, J.G.R. Hurrell, Curr. Protocols Mol. Biol. (2000)11.1.1–11.1.7.
[42] X. Chen, C. Ruan, J. Kong, J. Deng, Fresenius' J. Anal. Chem. 367 (2000) 172–177.
[43] S. Liu, J. Tian, L. Wang, G. Chang, X. Sun, Analyst 136 (2011) 4894–4897.
[44] J. Salonen, R. Vainionpaa, P. Halonen, Arch. Virol. 91 (1991) 93–106.
[45] T. Ruzgas, E. Csoregi, J. Emneus, L. Gorton, G.M. Varga, Anal. Chim. Acta 330 (1996) 123–138.
[46] R. Polsky, J.C. Harper, D.R. Wheeler, S.M. Dirk, D.C. Arrango, S.M. Brozik, Biosens. Bioelectron. 23 (2008) 757–764.
[47] G.K. Ahirwal, C.K. Mitra, Biosens. Bioelectron. 25 (2010) 2016–2020.
[48] Z.-P. Chen, Z.-F. Peng, P. Zhang, X.-F. Jin, J.-H. Jiang, X.-B. Zhang, G.-L. Shen, R.-Q. Yu, Talanta 72 (2007) 1800–1804.
[49] I.O. Okonko, A.O. Nkang, A.O. Udeze, A.O. Adedeji, J. Ejembi, B.A. Onoja, A.A. Ogun, K.N. Garba, J. Cell Anim. Biol. 3 (2009) 119–140.
[50] S. Verguet, W. Jassat, C. Hedberg, S. Tollman, D.T. Jamison, K.J. Hofman, Vaccine 30 (2012) 1594–1600.